Design and Analysis of Sandwiched Stator Axial Flux Permanent Magnet Brushless DC Motor

By

Dhruvesh M Jadav

12MEEP10

DEPARTMENT OF ELECTRICAL ENGINEERING

AHMEDABAD-382481

May 2014

Design and Analysis of Sandwiched Stator Axial Flux Permanent Magnet Brushless DC Motor

Major Project Report

Submitted in Partial Fulfillment of the Requirements for the Degree of

MASTER OF TECHNOLOGY

IN

ELECTRICAL ENGINEERING

(Power Electronics, Machines & Drives)

By

Dhruvesh M Jadav

12MEEP10

DEPARTMENT OF ELECTRICAL ENGINEERING

INSTITUTE OF TECHNOLOGY

NIRMA UNIVERSITY

AHMEDABAD-382481

May-2014

Certificate

This is to certify that the Major Project Report entitled **"Design and Analysis of Sandwiched Stator Axial Flux Permanent Magnet Brushless DC Motor"** submitted by **Mr.Dhruvesh M Jadav (Roll No: 12MEEP10)** towards the partial fulfillment of the requirements of Master of Technology (Electrical Engineering) in the field of Power Electronics, Machines & Drives of Nirma University is the record of work carried out by him under our supervision and guidance.The work submitted has in our opinion reached a level required for being accepted for examination. The results embodied in this major project work to the best of our knowledge have not been submitted to any other University or Institution for award of any degree or diploma.

Date:

.....

Institute Guide

Prof. A. N. Patel

Department of Electrical Engineering

Institute of Technology

Nirma University

Ahmedabad.

.....

Co-Guide

Prof. T. H. Panchal

Department of Electrical Engineering

Institute ofTechnology

Nirma University

Ahmedabad.

Head of Department

Department of Electrical Engineering

Institute of Technology

Nirma University

Ahmedabad

Director

Institute of Technology

Nirma University

Ahmedabad

Undertaking for Originality of the Work

I, Dhruvesh M Jadav, Roll No. 12MEEP10, give undertaking that the Major Project entitled "Design and Analysis of Sandwiched Stator Axial Flux Permanent Magnet Brushless DC Motor" submitted by me, towards the partial fulfilment of the requirements for the degree of Master of Technology in Power Electronics, Machines & Drives, Electrical Engineering, under Institute of Technology of Nirma University, Ahmedabad, Gujarat is the original work carried out by me and I give assurance that no attempt of plagiarism has been made. I understand that in the event of any similarity found subsequently with any published work or any dissertation work elsewhere, it will result in severe disciplinary action.

.....

Signature of student

Date:.....

Place:.....

.....

Institute Guide

Prof. A. N. Patel

Department of Electrical Engineering

Institute of Technology

Nirma University

Ahmedabad.

.....

Institute Co-Guide

Prof. T. H. Panchal

Department of Electrical Engineering

Institute of Technology

Nirma University

Ahmedabad.

Acknowledgements

My sincere appreciation goes to my Guide Prof. A. N. Patel and my Co-Guide Prof. T. H. Pacnchal, for all I have learned from them and for their continuous help and support in all stages of my project. I would also like to thank him for being an open person to ideas, and for encouraging and helping me to shape my interest and ideas. I would also like to thank our Director of Institute of Technology Dr. K. Kotecha and head of Electrical Engg. department Prof. Dr. P.N Tekwani for providing the infrastructure to pursue the project in-house. I am also thankful to all those who have helped me directly or indirectly during my project. I would thank my mother for suporting me everytime.

Dhruvesh M Jadav
12MEEP10

Abstract

Axial-flux permanent-magnet machines are important technology in many applications, where they are an alternative to radial-flux permanent-magnet machines. There are many technological advancements in axial-flux permanent-magnet machines, in aspects of construction, features, modeling, simulation, analysis and design procedure. Axial-flux permanent-magnet (AFPM) machines have many unique features. For being permanent magnet, they usually are more efficient, as field excitation losses are eliminated, reducing rotor lossses significantly. Machine efficiency is thus greatly improved, and higher power density achieved. Axial-flux construction has less core material, so, high torque-to-weight ratio. Also, AFPM machines have thin magnets, so are smaller than radial flux counterparts. AFPM machine size and shape are important features in applications where space is limited, so compatiblity is crucial. The noise and vibration they produce are less than those of conventional machnes. Their air gaps are planar and easily adjustable. These benefits give AFPM machines advantages over conventional machines, in various applications. Computer aided design procedure of Axial Flux Permanent Magnet Brushless DC Motor is done. Subsequently analysis and performance estimation is carried out.

List of Figures

Contents

Nomenclature

T = Torque N-m

N = Rated speed rpm

E_{max} = Back emf v

J_{max}= Maximum slot current denstiy A/m_2

N_{ph} = Number of pahses

N_m = Number of magnet poles

N_{sp} = Number of slots per phase

g = Lenght of air gap m

l_m = Magnet lenght m

R_o = Ouster Radius m

R_i = Inner Radiux m

k_{st} = Stacking factor

k_{cp} = Conductor packing factor

τ_f = Magnet spacer width m

B_r = Magnet remanance T

μ_r = Magnet recoil permeability

B_{max} = Maximum flux density T

w_s = Slot opening

α_{sd} = Shoe depth fraction

ω_m = Mechanical speed rad/s

ω_e = Electrical speed rad/s

N_s = Number of slots

N_{spp} = Number of slots per pole per phase

N_{sm} = Number of slots per pole

α_{cp} = Coil-pole fraction

θ_p = Angular pole pitch

θ_s = Angular slot pitch

θ_{se} = Angular slot pitch

τ_{pi} = Inside pole pitch

τ_{po} = Outside pole pitch

τ_{ci} = Inside coil pitch

τ_{co} = Outside coil pitch

τ_{si} = Inside slot pitch

k_d = Distribution factor

k_p = Skew factor

α_m = Magnet fraction

C_ϕ = Flux concentration factor

P_c = Permeance coefficient

k_{ml} = Magnet leakage factor

g_c = Effective air gap for Carter coefficitent

k_c = Carter coefficient

A_g = Air gap area

B_g = Air gap flux density

ϕ_g = Air gap flux

w_{bi} = Back iron width

w_{tbi} = Tooth width at inner radius

$w_s - b$ = Slot bottom width

α_{si} = Slot aspect ratio at inner radius

N_s = Number of turns per slot

I_s = Peak slot current

I_{ph} = Phase current

d_3 = Conductor slot depth

A_s = Conductor area

J_c = Peak conductor current density

d_s = Total slot depth

L = Axial length

B_{smax} = Peak slot flux density

R_s = Slot resistance

R_c = End turn resistance

R_{ph} = Phase resistance

L_g = Air gap Inductance

L_s = Slot leakage inductance

L_e = End turn Inductance

L_{ph} = Phase inductance

V_{st} = Stator steel volume

Chapter 1

Introduction

1.1 Electric Motor Development

Intially motors were developed in mid 1800 and these motors were DC motors. William Sturgeon was the first to make commutator DC electric motor. Followed by Sturgeon's work Thomas Davenport built a commutator-type direct-electric current electric motor for commercial use. These motors were used for powering machine tools and printing press. But because of high cost of battery these motors were commercially unsuccessful.

Practical rotating AC induction motors were independently invented by Galileo Ferraris and Nikola Tesla, a working motor model having been demonstrated by the former in 1885 and by the latter in 1887. In 1888, Tesla presented his paper ***A New System for Alternating Current Motors and Transformers*** to the AIEE that described three patented two-phase four-stator-pole motor types: one with a four-pole rotor forming a non-self-starting reluctance motor, another with a wound rotor forming a self-starting induction motor, and the third a true synchronous motor with separately excited DC supply to rotor winding.[9]

1.1.1 Basic motor types for first 75 years

- DC motors (wound rotor and commutated)
  - Battery powered
  - DC supply
- AC motors powered with 50-60 Hz grid
  - AC Induction and AC Synchronous

1.1.2 Motor types from most recent 50 years

- Electronically controlled for variable speed motors are
  - Stepper motors
  - Permanent Magnet Brushless motor and Permanent Magnet-AC synchronous motor
  - AC Induction motor, Variable Frequency and flux vector controlled motors
  - Reluctance Synchronous Motor
  - Radial flux permanent magnet motor, Axial flux permanent magnet motor and Transverse Flux motor

1.2 Classification Chart for Motors

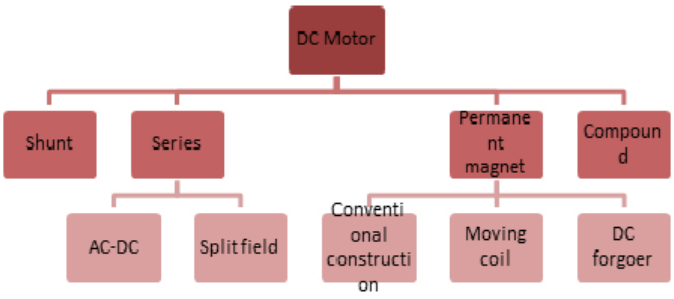

Figure 1.1: DC Motor

Figure 1.2: AC Motor

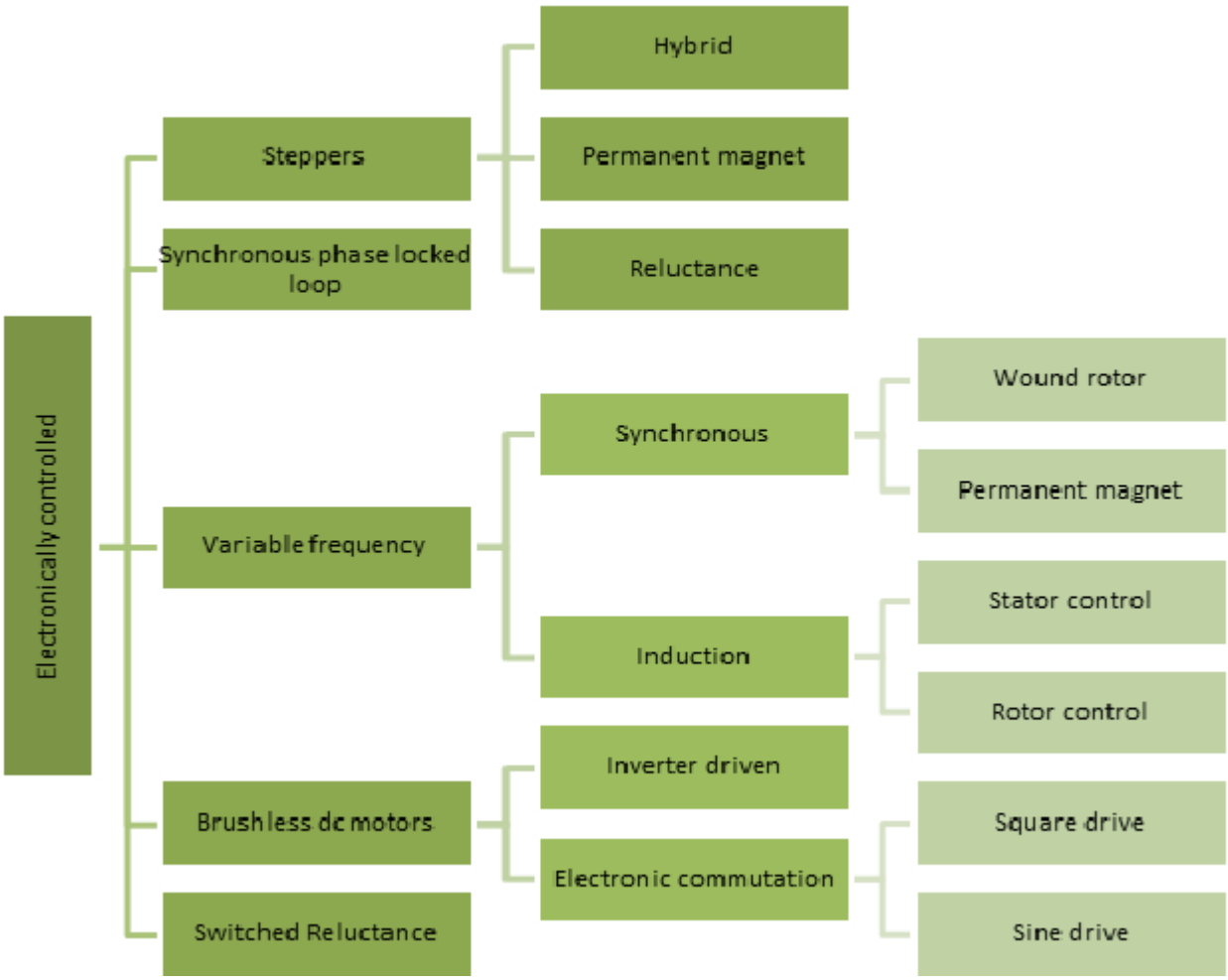

Figure 1.3: Electronically controlled Motor

1.3 Development of Axial Flux Permanent Magnet AFPM machines

The history of electrical machines reveals that the earliest machines were axial flux machines (M. Faraday, 1831, anonymous inventor with initials P.M., 1832, W. Ritchie, 1833, B. Jacobi, 1834). However, shortly after T. Davenport (1837) claimed the first patent for a radial flux machine, conventional radial flux machines have been widely accepted as the mainstream configuration for electrical

machines. [7] The reasons for not using the axial flux machine were many and can be summarized as follows:

- Axial magnetic attractive force between the stator and rotor is very strong
- In these motors the slots are to be cut in laminated cores so fabrication difficulties occur.
- Methods of making slotted stator cores.
- As laminated stator cores are to be formed there is high cost of manufacturing.
- Due to high magnetic force between stator and rotor assembling of the machine and maintaining uniform air gap is difficult.

Earlier the Permanent magnet excitation was applied to electrical machines but due to the lower quality of hard magnetic materials their use was not encouraged. But the invention of magnetic materials like Alnico, barium ferrite and the rare-earth magnetic material like neodymium-iron-born(NdFeB) the use of Permanent magnet excitation have become popular.

It is beleieved that the due to the presence and availability of high energy of Permanent magnet materials novel permanent magnet machine topoligies are developed and Axial flux Machines were thus developed. Also the prices of rare earth permanent magnet materials are decreasing in the last decade. The prices of rare earth permanent magnets are such that their price per kilogram is less. So axial flux machines will play importnt role as the prices of permanent magnet materials is being affordable.[7]

1.4 Features

The Axial Flux PM machine, also called the disc-type machine, is a very suitable alternative to the cylindrical Radial Flux PM machine due to its pancake

shape, compact construction and high power density. AFPM motors are particularly suitable for electrical vehicles, pumps, fans, valve control, centrifuges, machine tools, robots and industrial equipment. The large diameter rotor with its high moment of inertia can be utilized as a flywheel. Axial Flux PM machines can also operate as small to medium power generators. Since a large number of poles can be accommodated, these machines are ideal for low speed applications, as for example, electromechanical traction drives, hoists or wind generators.

The unique disc-type profile of the rotor and stator of Axial Flux PM machines makes it possible to generate diverse and interchangeable designs. Axial Flux PM machines can be designed as single air gap or multiple air gaps machines, with slotted, slot less or even totally ironless armature. Low power Axial Flux PM machines are frequently designed as machines with slot less windings and surface Permanent Magnets.

As the output power of the Axial Flux PM machines increases, the contact surface between the rotor and the shaft in proportion to the power becomes smaller. Careful attention must be given to the design of the rotor-shaft mechanical joint as this is usually the cause of failures of disc type machines. In some cases, rotors are embedded in power-transmission components to optimize the number of parts, volume, mass, power transfer and assembly time. For electric vehicles (EVs) with built-in wheel motors the payoff is a simpler electromechanical drive system, higher efficiency and lower cost. Dual function rotors may also appear in pumps, elevators, fans and other types of machinery, bringing new levels of performance to these products. Most applications use the Axial Flux PM machine as a DC brushless motor. Encoders, resolvers or other rotor position sensors are thus a vital part of brushless disc motors. [7]

1.5 Types of axial flux PM machines

In principle, each type of a radial flux machine should have its corresponding axial flux (disc type) version. In practice, disc type machines are limited to the following three types:

- Permanet Magnet DC commutator machines
- Permanent Magnet brushless DC and synchronous machines;
- Induction machines

Similar to its RFPM counterpart, the Axial Flux PM DC commutator machine uses Permanent Magnets to replace the electromagnetic field excitation system. The rotor (armature) can be designed as a wound rotor or printed winding rotor.

1.6 Topologies and geometries

From construction point of view, brushless Axial Flux PM machines can be designed as single-sided or double-sided, with or without armature slots, with or without armature core, with internal or external PM rotors, with surface mounted or interior PMs and as single stage or multi-stage machines.

In the case of double-sided configurations, either the external stator or external rotor arrangement can be adopted. The first choice has the advantage of using fewer PMs at the expense of poor winding utilisation while the second one is considered as a particularly advantageous machine topology. The diverse topologies of AFPM brushless machines may be classified as follows:

- Single-sided Axial Flux PM machines
  - With slotted stator
  - With slotless stator

    - With salient-pole stator
    - With salient pole stator

- With internal rotor
    - With slotted stator
    - With slotless stator
    - With salient pole stator

- Multi-stage (multidisc) Axial Flux PM machines

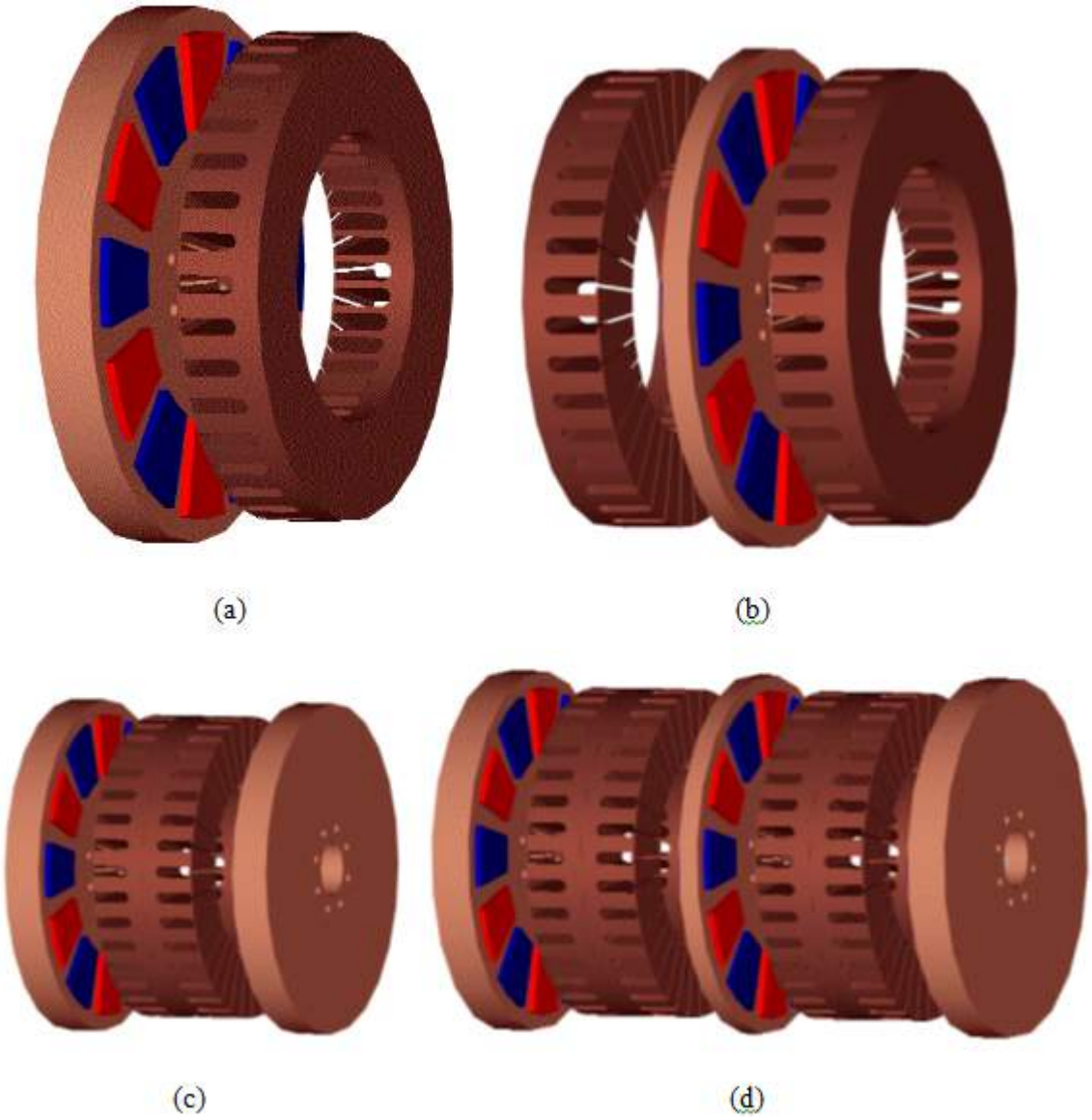

a) Single Stator Single Rotor

b) Sandwiched Rotor

c) Sandwiched Stator

d) Multi-disc arrangement

1.7 Comparison of Radial Flux PM machine and Axial Flux PM machine

Radial Flux Permanent Magnet (RFPM) Machine

Conventional radial flux PM machines have now been used extensively for decades. Many papers exist in the literature concerning the RFPM machine, the most common type of PM machine used in industry. These machines are well known to have higher torque capability than the more common induction machine (IM). The efficiency is also higher than an IM due to the lack of rotor windings have higher power density and higher torque per ampere ratio. The main disadvantage of the RFPM is that during manufacturing the permanent magnet should be carefully fitted such that the rotor does not fly apart.

The non-slotted version of the conventional radial flux PM machine has also been analyzed in the literature. The two major differences between the slotted and non-slotted versions of the radial flux PM machine are the existence of slots and the type of polyphase winding. The stator structure is non-slotted and consists of a stack of laminated steel. Back-to-back connected polyphase windings are wrapped around the stator in a toroidal fashion and termed air gap windings since the windings are not placed into slots. The places in between the windings are filled with epoxy resin to increase robustness and provide better conductor heat transfer. The rotor structure is formed by surface mounted NdFeB magnets, rotor core and shaft.

It should be noted that only the windings facing the rotor Permanent Magnets are used for torque production in RFPMs. The portions of the windings on the outside surface of the stator and the portions on both sides are considered to be end windings in this topology. Therefore, this topology has long end windings when the aspect ratio D/L (diameter over axial length) is small. There wil be high copper loss if aspect ratio si small. Also, the flux density is reduced due

to the large air gap. The important advantage of this Radial Flux machine is that the heat transfer from the stator frame is very easily done. So the machine electrical loading can be relatively high.

Axial Flux Permanent Magnet (AFPM) Machine

The first work focused on PM disc machines was performed in late 70s and early 80s. Disc type axial flux PM machines have found growing interests in the last decade especially in the 90s and have been increasingly used in both naval and domestic applications as an alternative to conventional radial flux machines. As briefly mentioned earlier, AFPMs have some distinct advantages over RFPMs. First, that they can be designed to have a higher power-to-weight ratio so the core material used will be less and efficiency would be higher. Secondly, that axial flux machines are smaller in size than the radial flux machines and have disc shaped rotor and stator structures. This is an important feature of axial flux machines because suitable shape and size to match the space limitation is crucial for some applications such as electric vehicle.

Thirdly, axial flux machines have planar and adjustable airgaps, whereas radial flux machines dont have. Moreover, the direction of the main airgap flux can be varied and many discrete topologies can be derived. For instance, while the main flux traveling axially through the air gap and stator core creates an external-rotor internal- stator topology, the main air gap flux traveling axially through the airgap and both axially and radially in the stator core creates a second external-rotor-internal stator topology. These features provide the AFPMs with certain advantages over conventional RFPMs in some applications.[7]

Both radial and axial flux machines can be constructed in many ways. They can be constructed in single-stator-single-rotor form or multiple-stator multiple-rotor form. Axial flux machines are classified based on the rotor structure. It is termed an axial flux induction machine if the rotor structure is a squirrel cage; an axial flux surface mounted permanent magnet machine if the rotor is formed

by surface mounted permanent magnets; and an axial flux interior PM machine if the rotor has an interior magnet structure. The focus will be on axial flux surface mounted PM machines with different rotor configurations but there will be a short review of some other type of AFPMs and applications as well.

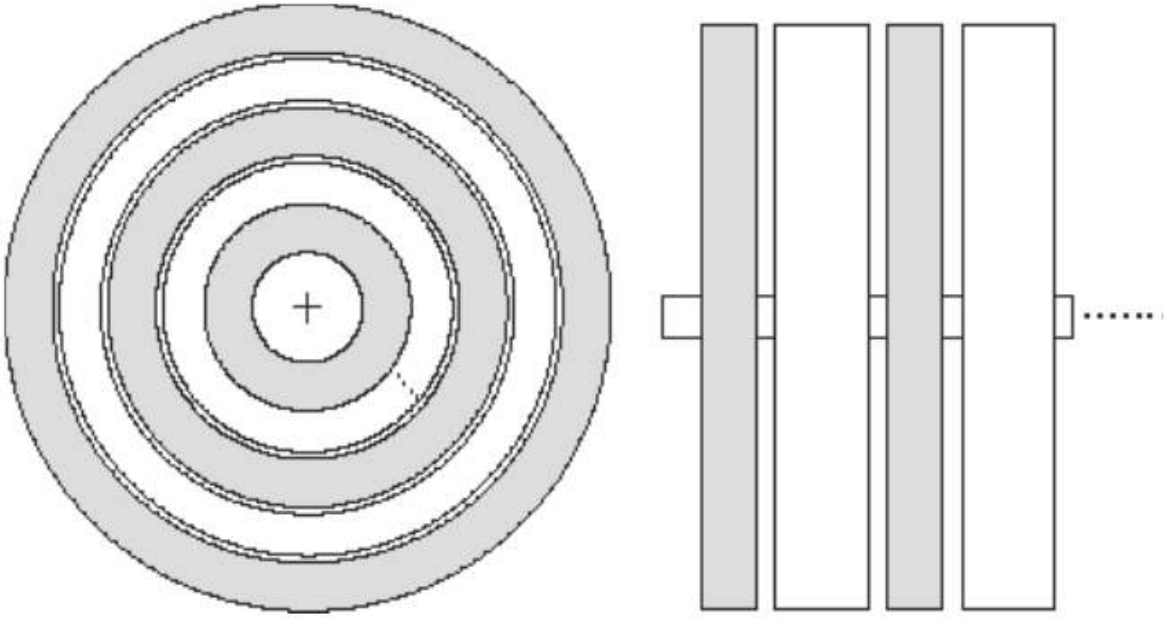

Figure 1.4: Radial and Axial Flux machines in multistage form

1.8 Scope of work

The proposed project focuses on the design Sandwiched Stator Axial Flux Permanent Magnet Brushless DC Motor.

- Computer Aided Programmng for motor design
- Modelling of the design in Finite Element Software
- Fininte element analysis of the design
- Comparison of the model designed Finite Element Analysis software and Computer aided Programming

1.9 Literature survey

The objective of this paper is to examine the AFPMs covered in the literature and investigate several new and promising AFPM structures. A total review about Radial Flux Permanent Magnet and Axial Flux Permanen Magnet motors. Axial flux surface magnet PM machines including slotless and slotted topologies with different number of rotor and stators are extensively reviewed. A general look at the AFPMs other than surface magnet Permanent Magnet (PM) structures is also presented. Sizing and design approach is briefly summarized as well. Some flux weakening PM topologies from a machine design point of view are also reviewed[1]

The computer-aided design and analysis of a pancake-type three-phase axial-field permanent magnet brushless dc motor meant for the direct drive of an electric two-wheeler is presented. The motor has been designed for accommodating inside the rim of the wheel. Initially, the motor design was carried out using the conventional procedure. Then three-dimensional finite element analysis was carried out to arrive at the optimum design by tuning the geometry to achieve the best utilization of all materials used. The effects of all machine

parameters on performance of the motor have been studied in detail and the results of this parametric study are provided. The entire design procedure is explained with the help of a flow chart. All steps involved in the design of the motor such as selection of the configuration, design of the magnetic circuit, selection of materials, calculation of machine parameters, and calculation of performance are discussed.[2]

This is reference book title Brushless Permanent Magnet And Reluctance Motor Drives. A very good explanation about the basics of control for PMBLDC and PMSM motors is given in this book. Also the basics of permanent magnet material is discussed in this book.[3]

This paper titled A comparison of Radial Axial PM synchronous motor In this paper comparison of Radial flux and Axial flux permanent magnet synchronous motor gives lot reasons for comparison between RFPM AFPM motor. Difference between both on the base of performance and working is explained.[4]

This is reference book titled Brushless Permanent Magnet Motor Design. In this book basics of PM motor has been discussed in detailed. The design procedure is very well explained in this book. In this book a design for rotor sandwiched between two stators geometry has been discussed. Design for axial flux permanent magnet motor has been done in this project by taking this book as main refernce.[5]

The effect of variation of design schemes is investigated for the reduction of cogging torque and increase of average torque. In other to examine the effects of slot shapes and the slot skewing on the cogging torque. 3D Finite Element Analysis (FEA) software is used for the accurate magnetic field analysis and the validity of the analysis results is clarified by comparison between the simulated results and measured one. From the results, when the asymmetric skewed angle with 10 degree, we can improve the cogging torque and average torque characteristics. The paper shows the reduction of cogging torque in a novel axial flux

permanent magnet (AFPM) motor through the various design schemes. 3D finite element method is used for the exact magnetic field analysis. The effects of slot shapes and skewing of slot on the cogging torque and average torque have been investigated in detail. The validity of the analysis results is also clarified by comparison between calculated results and measured ones.[6]

In this paper a novel integral force technique is introduced. This paper gives help to analyze any three dimensional model into two dimensions. Cutting and stretching of 3D model is done and then 2D FEA is carried out. By this method result error is increased but the time required is reduced.[8]

Chapter 2

Design of Axial Flux Permanent Magnet Brushless DC Motor

2.1 General Design process for electric machine design

1 Start with a specification including performance requirements and size

2 Select machine type, AC Induction machine,Brushless DC machine, Permanent Magnet AC machine

3 Establish number of poles (Choose if not in spec)

4 Assuming stator Outer diameter

5 Estimate rotor design (separate process for each motor type)

6 Select stator slots and phase windings

7 Select magnetic materials, (electricals steels, magnets, Cu vs. Al)

8 Estimate magnetizing flux and select turns per coil and wire guage

9 Finalize circuit cross sections, (yokes and teeth dimensions)

10 Solve for performance results (usually analytical equations or FEA)

2.2 Calculation of main dimesions

$$P_o = T\omega_m = \eta N_c E_{ph} I_{ph} \tag{2.1}$$

$$T = \frac{P_o}{\omega_m} = \frac{\eta N_c E_{ph} I_{ph}}{\omega_m} \tag{2.2}$$

$$= \frac{\eta N_c [\omega_m N_m N_{spp} K_w B_g n_s (R_o^2 - R_i^2)] I_{ph}}{\omega_m} \tag{2.3}$$

$$T = \eta N_c N_m N_{spp} K_w B_g I_s R_o^2 (1 - \frac{1}{K_r^2}) \tag{2.4}$$

$$T = \eta N_c N_m N_{spp} K_w B_g I_s R_o^2 \frac{2}{3} \tag{2.5}$$

$$R_o = \sqrt{\frac{3T}{2T N_c N_m N_{spp} K_w B_g I_s}} \tag{2.6}$$

$\mathrm{P}_o = Rated\ output\ power$

$\omega_m = Rated\ speed$

$T = Motor\ developed\ torque$

$\eta = Assumed\ efficiency\ of\ the\ motor$

$R_o = Outer\ radius\ of\ the\ stator$

$R_i = Inner\ radius\ of\ the\ stator$

$N_c = Number\ of\ coils\ conducting\ simultaneously$

$N_m = Number\ of\ poles$

$N_{spp} = Number\ of\ slots\ per\ pole\ per\ phase$

$K_w = Winding\ factor$

$B_g = Specific\ magnetic\ loading$

$n_s = Number\ of\ conductors\ per\ slot$

$K_r = Ratio\ of\ outer\ to\ inner\ diameter\ of\ the\ stator$

$I_{ph} = Phase\ current$

$I_s = Specific\ magnetic\ loading$

2.3 Magnetic Circuit

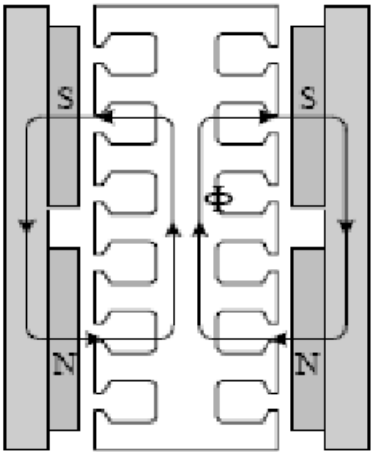

Figure 2.1: Dual airgap construction

From the above magnetic circuit it can be seen that the flux from the permanent magnets leaves North pole travels the air gap and then enters the stator through the slots from there it goes to the stator back iron and from there it goes to the South pole.

So while making an equivalent circuit three things are to be included rotor back iron R_r, air gap R_g and stator back iron R_s in the circuit. And some of the flux leakage from the North pole to the South pole without the above shown path, so magne leakage reluctance is to be added i.e. R_{ml}.

Thus we can model the circuit as shown in below figure, the two flux sources in the figure show the flux generated by the permanent magnet poles. Each pole is assumed to contribute half of the total air gap flux and hence the value of the flux source is $\phi_r/2$. Also the length of the air gap is assumed to be approximately twice due to

presence of the slots on the periphery hence the air gap reluctance becomes twice the nominal value (R_g).

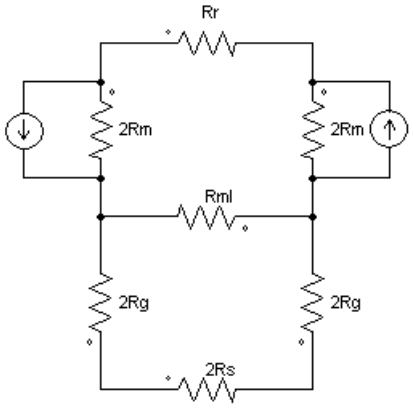

Figure 2.2: Equivalent magnetic circuit

Here the rotor and stator can be assumed to be infinitely permeable so we neglect the rotor reluctance (R_r) and stator reluctance (R_s) thus the circuit can be further reduced

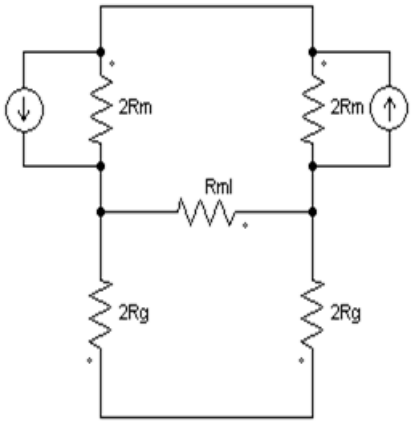

Figure 2.3: Modified magnetic circuit

The air gap reluctances can be combined to give following circuit

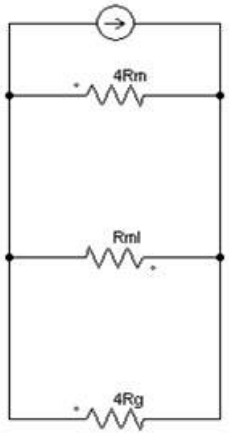

Figure 2.4: Modified magnetic circuit

Converting the equivalent reluctances to the permeances we get the final magnetic circuit

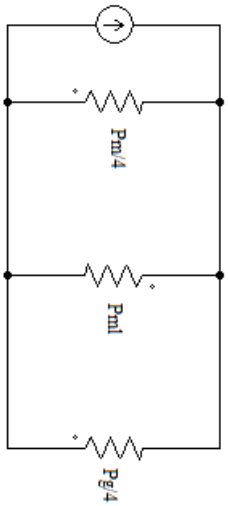

Figure 2.5: Final circuit

$$\frac{\phi_g}{2} = \frac{\frac{P_g}{4}}{\frac{P_g}{4} + \frac{P'_m}{4}} \frac{\phi_r}{2} \tag{2.7}$$

$$P_m = \frac{\mu_R \mu_o A_m}{l_m} \tag{2.8}$$

Where the magnet cross sectional area is

$$A_m = \alpha_m \frac{\pi}{N_m} (R_{out}^2 - R_{in}^2) \tag{2.9}$$

Where α_m is the magnet fraction for this topology

$$\alpha_m = 1 - \frac{N_m \tau_f}{\pi (R_{out}^2 + R_{in}^2)} \tag{2.10}$$

The magnet leakage permeance is given by the same expression determined as Radial flux machine with appropriate parameter changes for this topology,

$$P_{ml} = \frac{\mu_o (R_{out} - R_{in})}{\pi} ln(1 + \frac{\pi g}{\tau_f}) \tag{2.11}$$

Combining equation (2.9),(2.10) and (2.11) gives the effective permeance of

$$P'_m = P_m + 4P_{ml} = k_{ml} P_m \tag{2.12}$$

Where the magnet leakage factor k_{ml} is

$$k_{ml} = 1 + \frac{2P_{ml}}{P_m} = 1 + \frac{4 l_m N_m}{\pi^2 \mu_r \alpha_m (R_i + R_o)} ln[1 + \frac{\pi g}{\tau_f}] \tag{2.13}$$

Using the average of the areas, the air gap permeance is

$$P_g = \frac{\mu_o A_g}{g_e} \tag{2.14}$$

where $g_e = k_c$ g is the effective air gap length and k_c is some average Carter coefficient, and the air gap cross-sectional area is

$$A_g = \frac{\pi(1+\alpha_m)}{2N_m}(R_o^2 - R_i^2) \tag{2.15}$$

Substituting (2.8),(2.9),(2.12),(2.13),(2.14) in (2.7) air gap flux is

$$\phi_g = \frac{1}{1+\frac{4\mu_r\alpha_m k_{ml} k_c g}{(1+\alpha_m)l_m}}\phi_r \tag{2.16}$$

Flux concentration factor is

$$C_\phi = \frac{A_m}{A_g} = \frac{2\alpha_m}{1+\alpha_m} \tag{2.17}$$

and the permeance coeffiecient is $P_c = l_m/(2gC_\phi)$ because there are two airgaps in series so (2.16) can be written as

2.4 Geometric parameters

The magnet pole pitches at the inner and outer radii are

$$\tau_{pi} = R_i\theta_p \tag{2.18}$$

$$\tau_{po} = R_o\theta_p \tag{2.19}$$

where $\theta_p = 2\pi/N_m$ is the angular pole pitch and the associated coil pitches are

$$\tau_{ci} = \alpha_{cp}\tau_{pi} \tag{2.20}$$

$$\tau_{co} = \alpha_{cp}\tau_{po} \tag{2.21}$$

The slot pitches at the inner and outer radii are

$$\tau_{si} = R_i\theta_s \tag{2.22}$$

$$\tau_{so} = R_o\theta_s \tag{2.23}$$

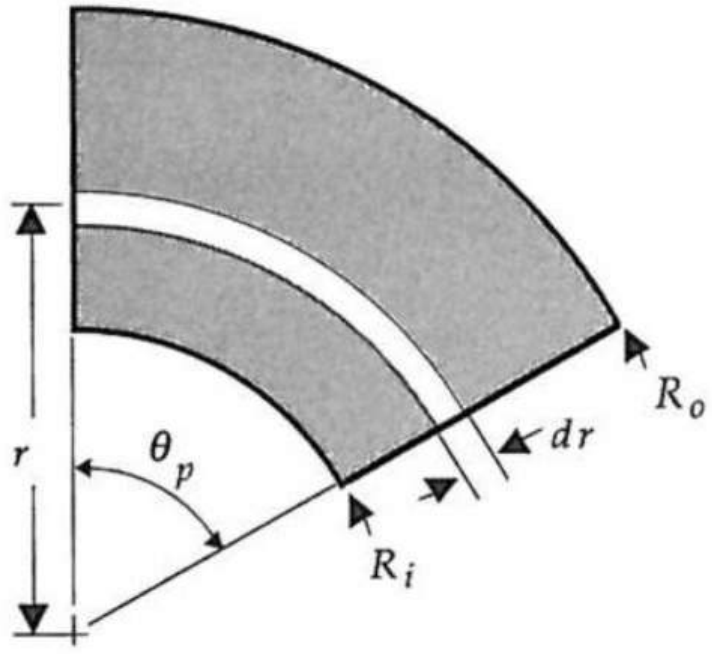

Figure 2.6: Slot geometry for the dual axial flux motor topology

where $\theta_s = 2\pi/N_s$ is the angular slot pitch.

The slot cross-sectional area available for conductors is rectangular and is given by

$$A_s = w_{sb} d_3 \tag{2.24}$$

where w_{sb} is the slot bottom width

2.5 Magnetic parameters

The magnetic parameters to be found are the stator back iron thickness and the stator tooth width. Since the magnet produces constant flux density over its surface, the total flux crossing the air gap increases linearly with radius due to

increasing magnet width. Thus the amount of flux to be supported by the stator back iron increases with radius To understand this phenomenon, consider the magnet shown in Fig. 2.7. The flux entering the stator from a differential slice is $\phi(r) = B_g \theta_p r dr$. In the stator, this flux splits in half in the back iron to return through adjacent magnets. Therefore, if B_{max} is the maximum allowable flux density in the back iron, the back iron flux is $\phi_{bi}(r) = B_{max} w_{bi} k_{st} dr$, from which the required back iron thickness

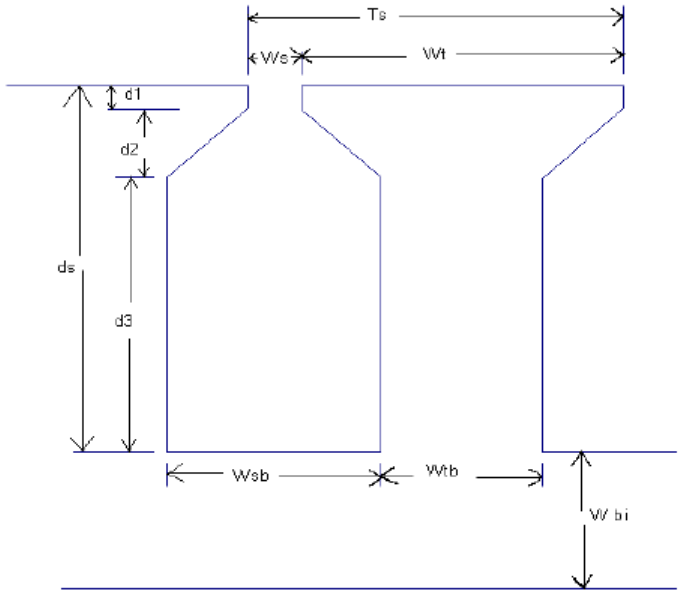

Figure 2.7: Geometry for the torque calculation in the dual axial flux motor topology

$$w_{bi}(r) = \frac{B_g \theta_p r}{2 B_{max} k_{st}} \tag{2.25}$$

It is not practical to build stators with a linearly increasing back iron width. Therefore, a constant back iron width equal to the maximum of (2.25) is chosen

$$w_{bi} = \frac{B_g \tau_{po}}{2 B_{max} k_{st}} \tag{2.26}$$

The require tooth bottom width is

$$w_{tb}(r) = \frac{2}{N_{sm}} w_{bi}(r) \tag{2.27}$$

$$w_{tbi} = \frac{B_g \tau_{pi}}{N_{sm} B_{max} k_{st}} \tag{2.28}$$

The above equation is for inner radius

Given (2.28) the slot bootom width is

$$w_{sb} = \tau_{si} - w_{tbi} \tag{2.29}$$

and the slot aspect ratio at the inner radius is

$$\alpha_{si} = \frac{w_{sb}}{w_{tbi} + w_{sb}} \tag{2.30}$$

As the slot opening has to find at the top of the slot it should be 20 percent to 30 percent of inner slot pitch

$$w_s = 0.2\tau_{si} \tag{2.31}$$

and the width of tooth at top is

$$w_{tti} = \tau_{si} - w_s \tag{2.32}$$

2.6 Torque

The torque produced by the axial flux topology requires some development because the torque is produced at a continuum of radii from R_i to R_o.

$$T = N_m k_d k_p k_s B_g L R_{ro} N_{spp} n_s i \tag{2.33}$$

L is the conductor length exposed to the air gap flux density B_g and R_{ro} is the radius at which torque is produced. Based on this equation the incremental torque produced at a radius r by the interaction of B_g and a conductor of length dr is from R_i to R_o.

$$T(r) = 2N_m k_d k_p k_s B_g N_{spp} n_s i r dr \tag{2.34}$$

the factor of 2 appears because there are conductors on two stators producing torque at the radius r. Integration of this incremental torque gives a total developed torque of

$$T = 2N_m k_d k_p k_s B_g N_{spp} n_s i \int_{R_i}^{R_o} r dr = N_m k_d k_p k_s B_g N_{spp} n_s i (R_o^2 - R_i^2) \tag{2.35}$$

R_o and R_i are the outer and inner radius respectievely

taking $\mathrm{K}_r = \frac{R_{out}}{R_{in}}$

maximum torque is achieved when $K_r = 1.73$

The torque is fixed quantity and also it is known. Thus the R_o is

$$R_o = \sqrt{\frac{3T}{2TN_c N_m N_{spp} K_w B_g I_s}} \tag{2.36}$$

2.7 Back emf

The equation of back emf is

$$e_{max} = \frac{T\omega_m}{i} = N_m k_d k_p k_s B_g N_{spp} n_s (R_o^2 - R_i^2)\omega_m \tag{2.37}$$

Therefore the number of turns per slot is

$$n_s = int[\frac{E_{max}}{N_m k_d k_s k_p B_g N_{spp} (R_o^2 - R_i^2)\omega_m}] \tag{2.38}$$

2.8 Current

$$I_s = \frac{T}{N_m k_d k_s k_p B_g N_{spp}(R_o^2 - R_i^2)} \tag{2.39}$$

$$I_{ph} = \frac{I_s}{N_{ph} n_s} \tag{2.40}$$

Given the specified maximum conductor current density J_{max} and the slot cross-sectional area (2.24), the conductor slot depth required to support Jmax

$$d_3 = \frac{I_s}{k_{cp} w_{sb} J_{max}} \tag{2.41}$$

2.9 Resistance

The slot resistance per slot is given by

From this the total stator axial length is calculated

$$R_s = \frac{\rho n_s^2 (R_o - R_i)}{k_{cp} A_s} \tag{2.42}$$

Since the end turn length is different at the inner and outer radii, the end turn resistance per slot is the average of that at the two radii,

$$R_e = \frac{\rho n_s^2 \pi (R_o - R_i)}{k_{cp} A_s} \tag{2.43}$$

Given two stators each having N_{sp} slots per phase, the phase resistance is

$$R_{ph} = 2N_{sp}(R_s + R_e) \tag{2.44}$$

2.10 Inductance

Calculation of the phase inductance requires slightly more work than the resistance because the air gap inductance is influenced by the two rotors and two air gaps.

$$L_g = \frac{n_s^2 \mu_R \mu_o \theta_c (R_o^2 - R_i^2) k_d}{4(l_m + 2\mu_R k_c g)} \tag{2.45}$$

$$L_s = n_s^2 \Big[\frac{\mu_o d_3}{3 w_{sb}} + \frac{\mu_o d_2}{(w_s + w_{sb})/2} + \frac{\mu_o d_1}{w_s} \Big] (R_o - R_i) \tag{2.46}$$

$$L_e = \frac{n_s^2 \mu_o \tau_{co}}{16} ln\Big(\frac{\tau_{co}^2 \pi}{4A_s}\Big) + \frac{n_s^2 \mu_o \tau_{ci}}{16} ln\Big(\frac{\tau_{ci}^2 \pi}{4A_s}\Big) \tag{2.47}$$

$$L_{ph} = 2N_{sp}(L_g + L_s + L_e) \tag{2.48}$$

2.11 Performance

$$V_{st} = 2k_{st}[\pi(R_o^2 - R_i^2)(w_{tbi} + d_s) - N_s A_s (R_o - R_i)] \tag{2.49}$$

The heat density leaving the slot conductors and the maximum heat density appearing at the stator periphery are

$$\eta = \frac{T\omega_m}{T\omega_m + P_r + P_{cl} + P_s} \tag{2.50}$$

Chapter 3

Computer aided design for Sandwiched Stator Axial Flux Permanent Magnet Brushless DC Motor

3.1 Introduction

To design an efficient and reliable drive system for a machine it is important to have a thorough knowledge of parameters of the machine. The parameters are so critical for the drive to perform efficiently such that they have to be estimated accurately and precisely.

3.2 Flow Chart

The following flow chart is for computer aided design of dual rotor Axial Flux Permanent Magnet Brushless DC motor.

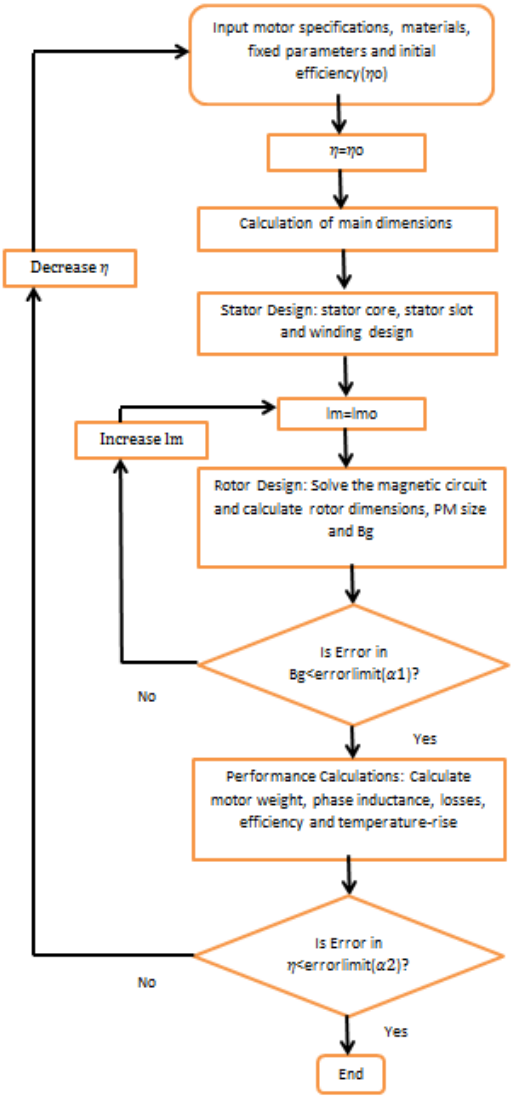

Figure 3.1: Flow chart for Computer aided program

The Flow chart shows that intially we have to give motor specifications, some fixed parameters and efficiency. In this the outer loop is for correcting the assumed efficiency and calculated efficiency. The correction takes place till the error between the assumed efficiency and calculated efficiency is within the limit. The inner loop is to minimize error between the assumed flux density and actual air gap flux density. There after stator design, rotor design and performance calculations are done. Since the scaling of the torque capability of the AFPM machine as the cube of the diameter while the torque of a RFPM machines scale as the square of the diameter times the length, the benefits associated with axial flux geometries may be lost as the power level or the geometric ratio of the length to diameter of the motor is increased. The transition occurs near the point where the radius equals twice the length of RFPM machine. This may be a limiting design consideration for the power rating of a single-stage disc machine as the power level can always be increased by simply stacking of disc machines on the same shaft and in the same enclosure.

After selection of motor topology some of the parameters should be assumed for the particular application. In this project low rating and low speed motor has been taken. For that here power rating of the motor is assumed to be 250 watt and 150 rpm with input voltage from battery is 48 V D.C. where supply frequency of the motor through the controller is 20 Hz. Where initial efficiency assumed to be 100%. Also number of other parameters should be assumed at initial calculation. After assuming all parameters main dimension is calculated.

3.3 Selection of Air Gap Flux Density (B_g)

Air gap flux density should be as high as possible, is needed for the desired torque production. For the permanent magnet motor flux is produced by the magnet. Length of the magnet highly affects flux density at air gap. Also higher length of magnet cause to increase overall cost of the motor and that is not permissible. Lower length of magnet cause to decreases mechanical strength of the magnet.Here in figure below variation of B_g v/s D_{out} given. If B_g varies between 0.45 to 0.85 then change in Dout is linear. Figure below shows variation of B_g v/s L_m (length of magnet) is given. If B_g is greater than 0.7 then change in length of magnet is much higher. And $B_g \leq$ 0.75 will give lower D_{out} which is quite helpful to increase efficiency and W/kg ratio is also increased

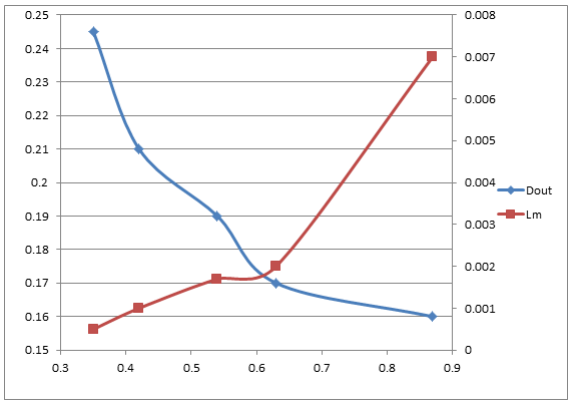

Figure 3.2: B_g vs D_{out}

3.4 Selection of Slot Loading (I_s)

Here motor armature has (Slot = N_{spp} * Poles * No.of phases = 1*16*3 = 48) slots as per the dimension. And for that each slot has loading within some limit. It should be less than 200 A/m for optimum design. If slot loading is very much lower than main dimensions are drastically changed. There are some limitation for selecting motor with very much higher aspect ratio (aspect ratio = D_{out}/L). If aspect ratio is very much higher than material used for the same rating is higher and also watt/kg ratio is decreased (it should be less than 250). Here in figure below the variation of slot loading on main dimension is given. As slot loading decreases the outer diameter (D_{out}) increases and as D_{out} increases, core losses increase but efficiency of the motor increases which is advantageous, for the all designers. But if the change in dimension is more than 30%, the efficiency will increase only by 1% then it should not be an optimum design.

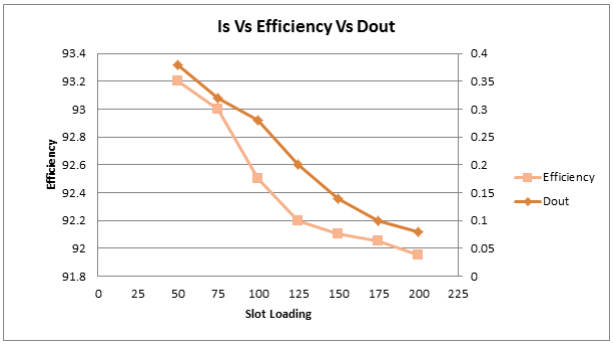

Figure 3.3: I_s vs D_{out}

3.5 Selection of Material

3.5.1 Rotor Core Material

Considering the behaviour as well as economic aspects, mild steel (low carbon steel) is selected as the rotor core material. This is done as the rotor core always carry a unidirectional flux produced by the permanent magnet and also as the effect of armature reaction is negligible owing to a large Air gap (the PM also act as an Air gap due to μ_r =1). Laminations are not required for the rotor core. Therefore a solid rotor core is considered, which will improve fabrication feasibility and mechanical strength.

Material	Mild Steel
Specific gravity	7.85 g/cc
Typical maximum relative permeability	2500
Saturation flux density	2.12 T

3.5.2 Stator Core Material

The important requirements for the stator material are high permeability, low hysteresis, and high resistivity. A various grades of silicon steel are available with different silicon content, which ranges from 0.5% to approximately 4.5%. For development of stator cold rolled grain oriented (CRGO) type material is available in Indian market. Cutting, shaping or machining of stator material most difficult subject.

Material	CRGO
Specific gravity	7.85 g/cc
Typical maximum relative permeability	2500
Saturation flux density	2.12 T

3.5.3 Permanent Magnet Material

Out of various types of permanent magnet materials commercially available as on day, Neodymium-Iron-Boron (NdFeB) is having highest energy product and also the highest residual flux density. The high remanence and coercivity of NdFeB material enables it appreciable reduction in motor frame size for the same output compared to other type of permanent magnet materials. As it is planned to have a compact, efficient and high power density, it is decided to use NdFeB permanent magnet, the magnetizing characteristics of NdFeB magnet is a straight line. The magnetic properties of which are given below.

Material	NdFeB
Coercieve force	-890 A/mm
Recoil permeability	1.05
Retentivity	1.23 T

The table for the specifications of the motor is as shown below

Specifications

Rated Power	P	250	Watt
Rated speed in rpm	N	150	rpm
Rated speed in rps	n	2.5	rps
Speed in $radian/sec$	ω_m	15.71	rad/s
No. of pahses	N_{ph}	3	
Supply voltage	V	48	Volt
No. of poles	N_m	16	

Assumed Data

Slot/pole/phase	N_{spp}	1	
No.of coils conducting simulataneously	N_c	2	
Winding Factor	K_w	0.96	
Ratio R_o/R_i	K_r	1.73	
Airgap flux density	B_g	.75	T
Specific slot loading	I_s	140	A/m
Magnet Spacer	τ_f	0.007	m
Length of Airgap	l_g	0.001	m
Magnet Recoil permeability	μ_r	1.0997	
Magnet remanance	B_r	1.2	T
Stacking factor	K_{st}	.9	
Maximum slot current density	J_{max}	$1e10^7$	A/m^2
Permeability	μ_o	$1.26e-6$	
Resistivity	ρ	$1.68e-8$	$\Omega - m$
Stacking factor	K_{st}	.9	

Output Data

Torque	T	15.9155	$N-m$
Number of slots	N_s	24	
Number of phases	N_{ph}	3	
Number of rotor poles	N_m	8	
Slot/pole/phase	N_{spp}	1	
Outer Diameter	R_o	0.1763	m
Inner Diameter	R_i	0.0772	m
Angular pole pitch	θ_p	0.7854	
Angular slot pitch	θ_s	0.2618	
Inside pole pitch	τ_{pi}	0.0291	
Outside pole pith	τ_{po}	0.0676	
Inside coil pitch	τ_{ci}	0.0291	
Outside coil pitch	τ_{co}	0.0676	
Inside slot pitch	τ_{si}	0.0097	
Distribution factor	k_d	1	
Ptich factor	k_p	1	
Skew factor	k_s	1	
Magnet sapcer	τ_f	0.007	
Magnet fraction	α_m	0.6365	
Flux concentration factor	C_ϕ	0.7779	
Length of Magnet	l_m	0.005	m
Length of airgap	g	$1e-3$	m
Permeance coefficient	P_c	3.2139	
Magnet recoil permeabilty	μ_r	1.0997	

Magnet leakage factor	k_{ml}	1.0349	
Effective airgap for Carter coefficient	g_c	0.0065	
Slot opening	w_s	0.0019	
Carter coefficient	K_c	1.0118	
Airgap area	A_g	0.0019	
Magnet remenance	B_r	1.2	
Air gap flux density	B_g	0.6872	
Airgap flux	ϕ_g	0.0013	
Back iron width	w_{bi}	0.0098	
Toooth width at inner radius	w_{tbi}	0.0037	
Slot bottom width	w_{sb}	0.0060	
Slot aspect ratio at inner radius	α_{si}	0.6182	
Conductor slot depth	d_3	0.0080	
Conductor area	A_s	$4.7987e-5$	

Chapter 4

Modelling & Analysis of Sandwiched Stator Axial Flux Permanent Magnet Brushless DC Motor

4.1 Introduction of Finite Element Analysis Software

In mathematics, the finite element method (FEM) is a numerical technique for finding approximate solutions to boundary value problems for differential equations. It uses variational methods (the calculation of variations) to minimize an error function and produce a stable solution. Analogous to the idea that connecting many tiny straight lines can approximate a larger circle, FEM encompasses all the methods for connecting many simple element equations over many small subdomains, named finite elements, to approximate a more complex equation over a larger domain.

4.2 MagNet

MagNet uses the finite element technique for an accurate and quick solution of Maxwell's equations. Each module is tailored to simulate different types of electromagnetic fields and is available separately for both 2D 3D designs.

4.3 Features

- Motion modeling supports multiple moving components with arbitrary direction (multiple degrees of freedom)
- Simulation results computed accurately and rapidly, increasing efficiency and productivity
- Circuit modeler for simulating loads and drives
- Easy to use intuitive interface for faster model building and analysis
- Integratable into any design process for multi-physics analysis
- Powerful parameterization capabilities available

4.4 Modelling & Analysis of Designed Motor

The Modelling of the motor is done according to dimensons from the CAD program from previous chapters. The designed motor has axial flux directions so the permanent magnet are mounted on rotor such that we get flux in axial direction. The current in the coil should be such that we get flux in axial directions. As per the requirement the model is designed in the Infolytica MagNet software so that further analysis can be carried out.

4.5 Winding Configuration

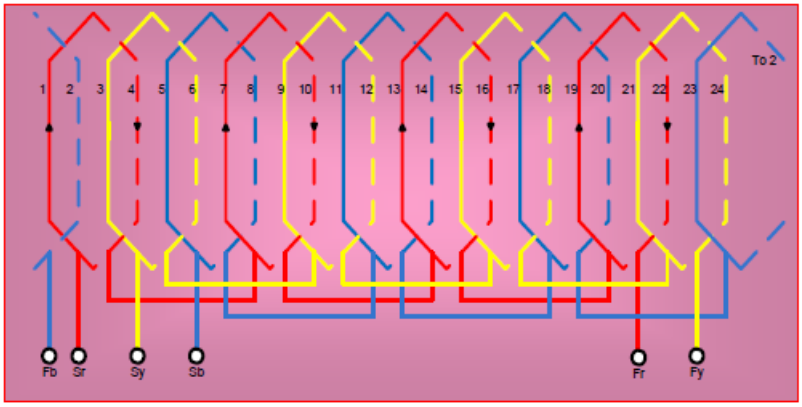

Figure 4.1: 24 Slots Stator Geometry

The above figure shows the winding configuration for 24 slot stator geometry. According to the winding configuration the coil should swept in the modelling software.

The winding for the modelled geometry is as shown below. The figure shows the

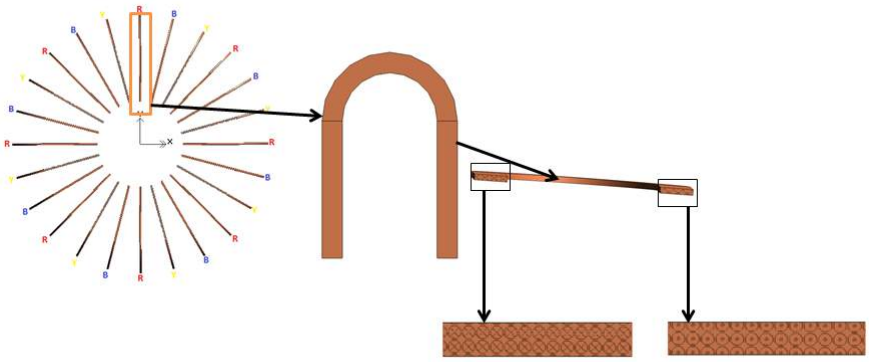

Figure 4.2: 24 Slots Winding Geometry

geometry of the coil the cross and dot shows the entry and exit of the current. Here the three phases are shown i.e. RYB.

The 24 slot stator geometry is as shown below.

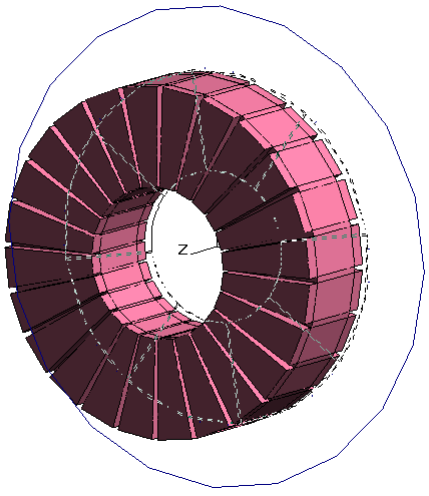

Figure 4.3: 24 Slots Stator Geometry

The 8 Pole rotor geometry is as shown below.

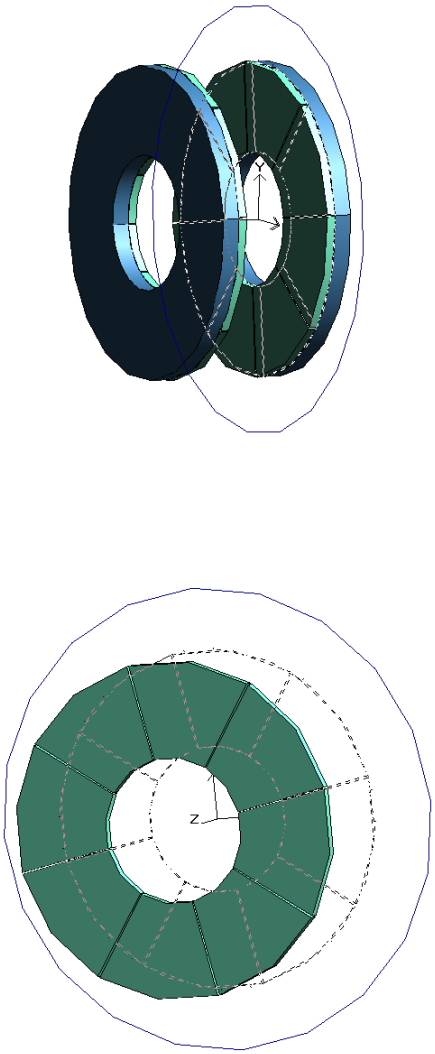

Figure 4.4: 8 pole rotor geometry

The full motor geometry is as shown below.

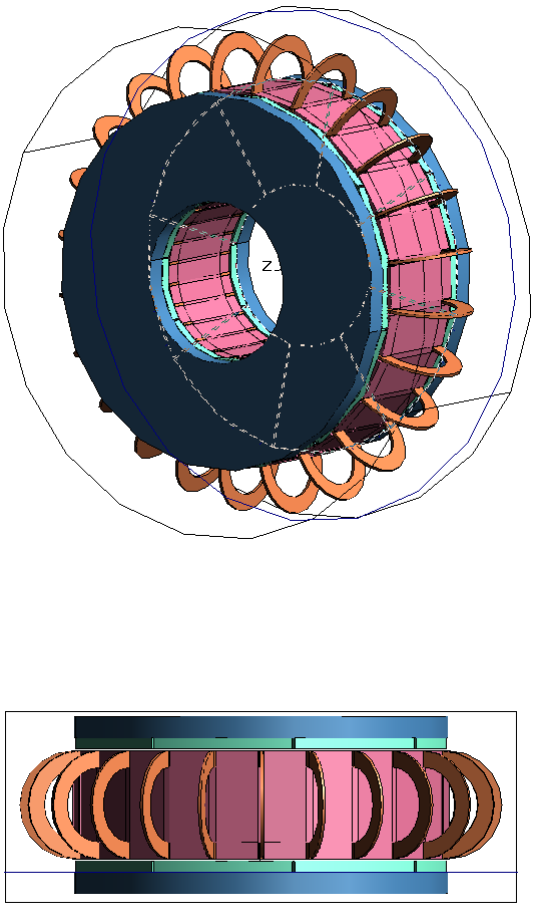

Figure 4.5: Full motor geometry

4.6 Excitation pattern for the Designed Model

Static analysis of the designed motor can be carried out by changing the rotor position and accordingly swithching the phases.

The 3D with motion analysis was not possible so a different approach was taken for finding the Average and Cogging torque. In this the excitations for two phases is given in the coil as shown in the figure 4.6, 4.7, 4.8, 4.9.

After every 15 degree mechanical the excitation changes for 1 phase the other phase remains the same. The switching changes after every 120 degree electrical i.e. 30 degree mechanical. According to the equation $\theta_e = \theta_m * No.of poles/2$ For every rotation of the rotor by 15 degree, excitation in the coil is changed as shown in the following figures. And the model is solved for that position. Here the solving of the model takes half hour for one position. By doing these till 45 degree we get the values for the torque and then the graph of the torque is plotted.

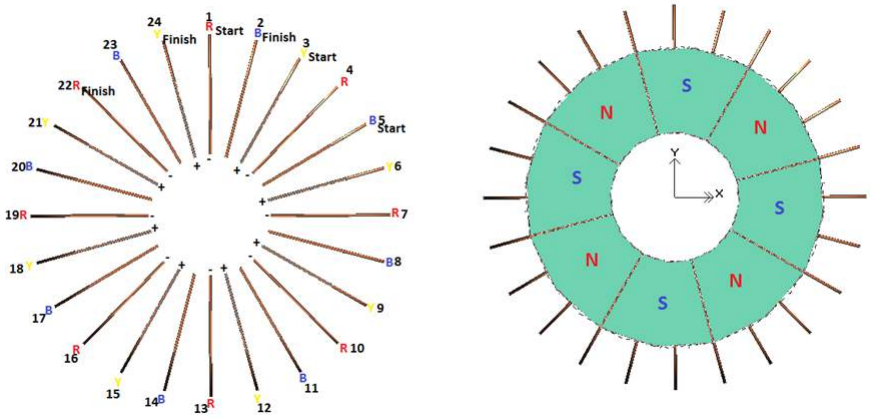

Figure 4.6: Excitation given for 0 Degree

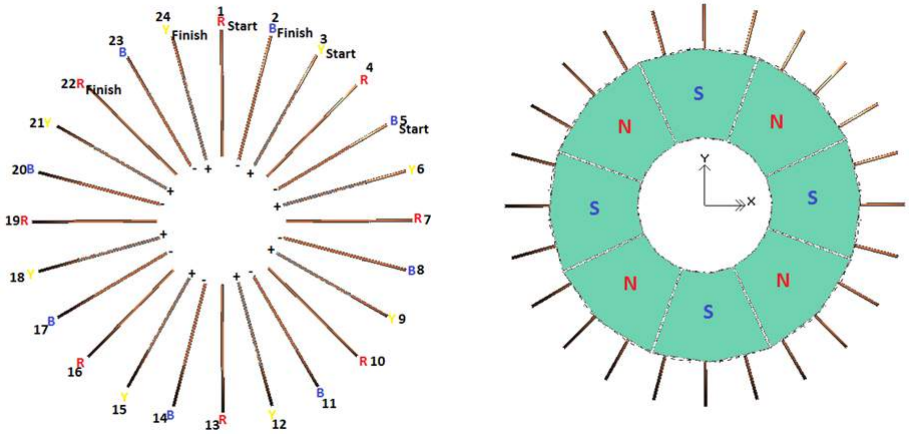

Figure 4.7: Excitation given for 15 Degree

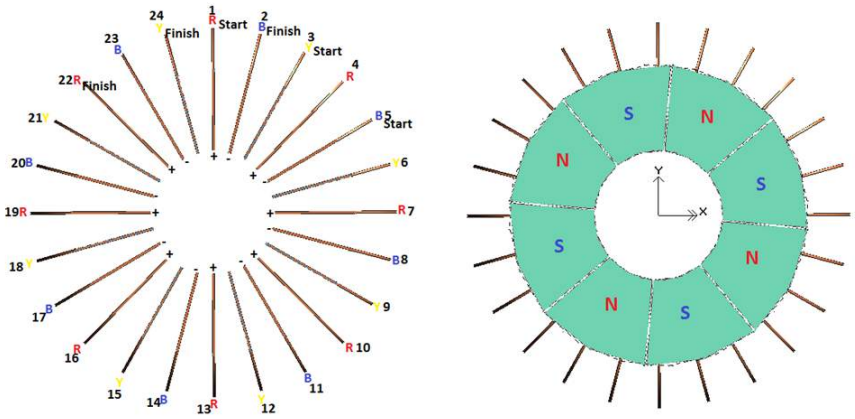

Figure 4.8: Excitation given for 30 Degree

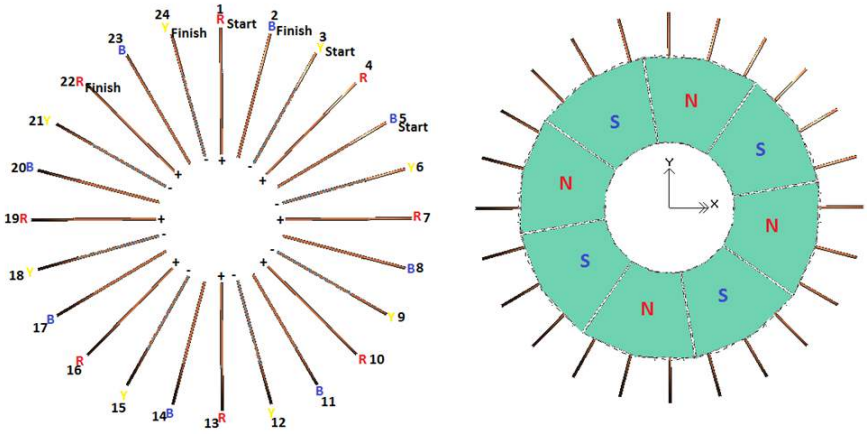

Figure 4.9: Excitation given for 45 Degree

The torque profile from the finite element analysis method is as shown in the below figure Figure shows graph of torque variation with respect to rotor position for one pole pitch. It will repeat for all poles as symmetrical model. By taking average of torque value average value can be obtained. From this FE analysis 15.371 Nm torque is obtained with 7.36% torque ripple.

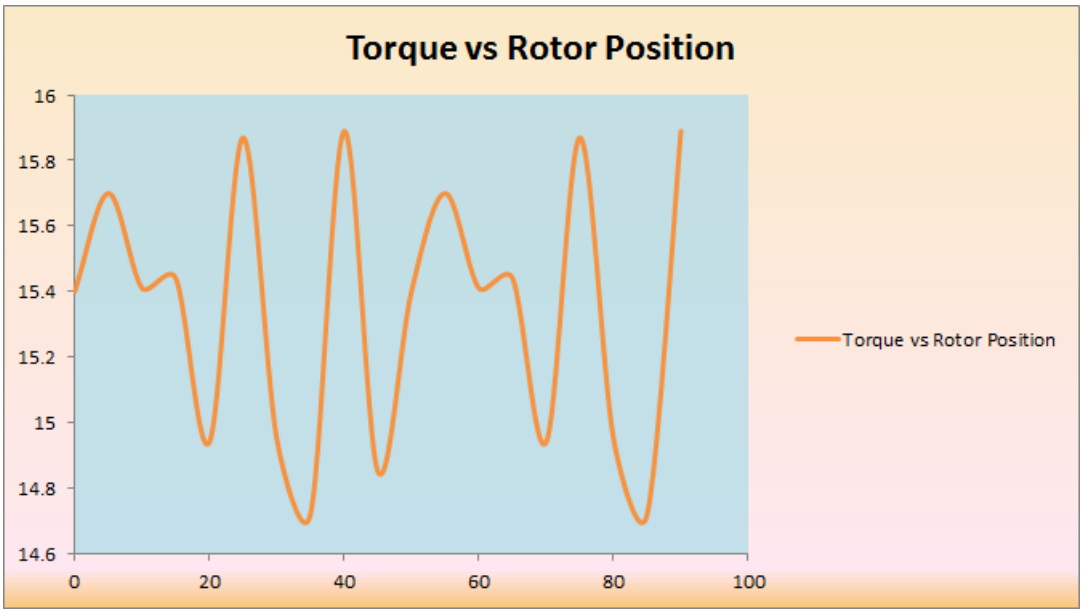

Figure 4.10: Average Torque profile

The cogging torque profile from the finite element analysis method is as shown in the below figure For cogging torque make the geometry without coil or define coil as an air material. Rotate rotor at one pole pitch after that the torque remains same. Figure shows the variation of cogging torque with respect to mechanical degree. In this case cogging torque is 0.99 Nm.

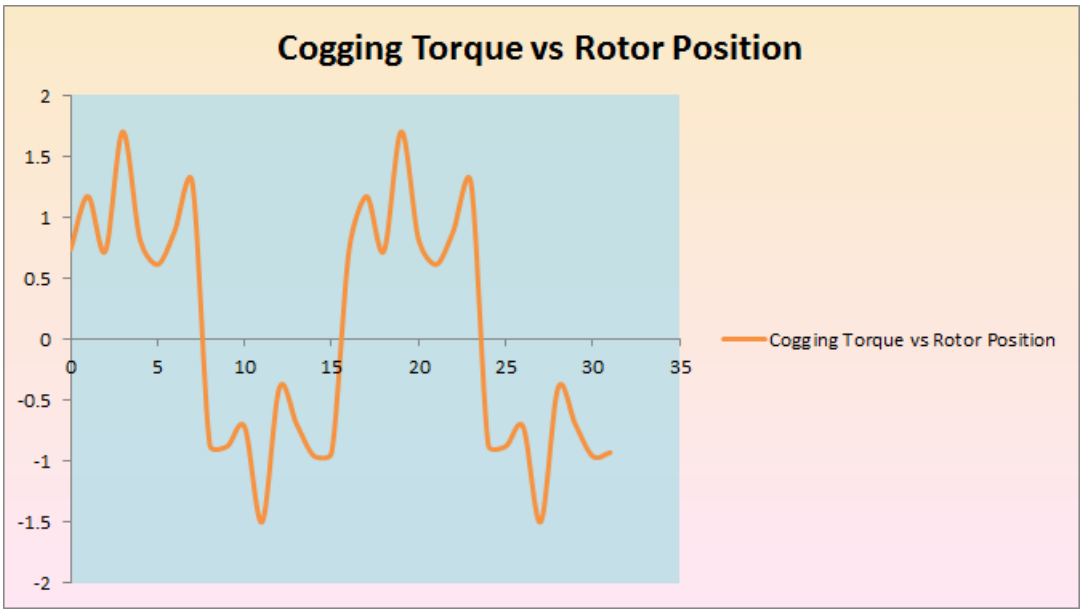

Figure 4.11: Cogging Torque profile

The intial 3D mesh of the model is as shown below

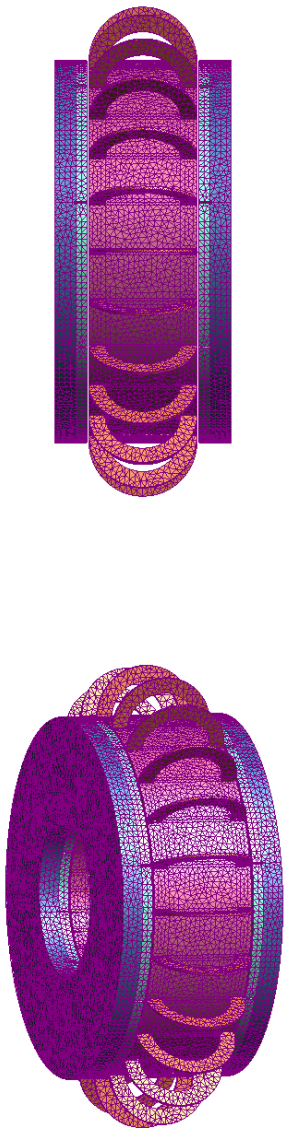

Figure 4.12: Intial 3D mesh

The flux density plot is given for the designed model

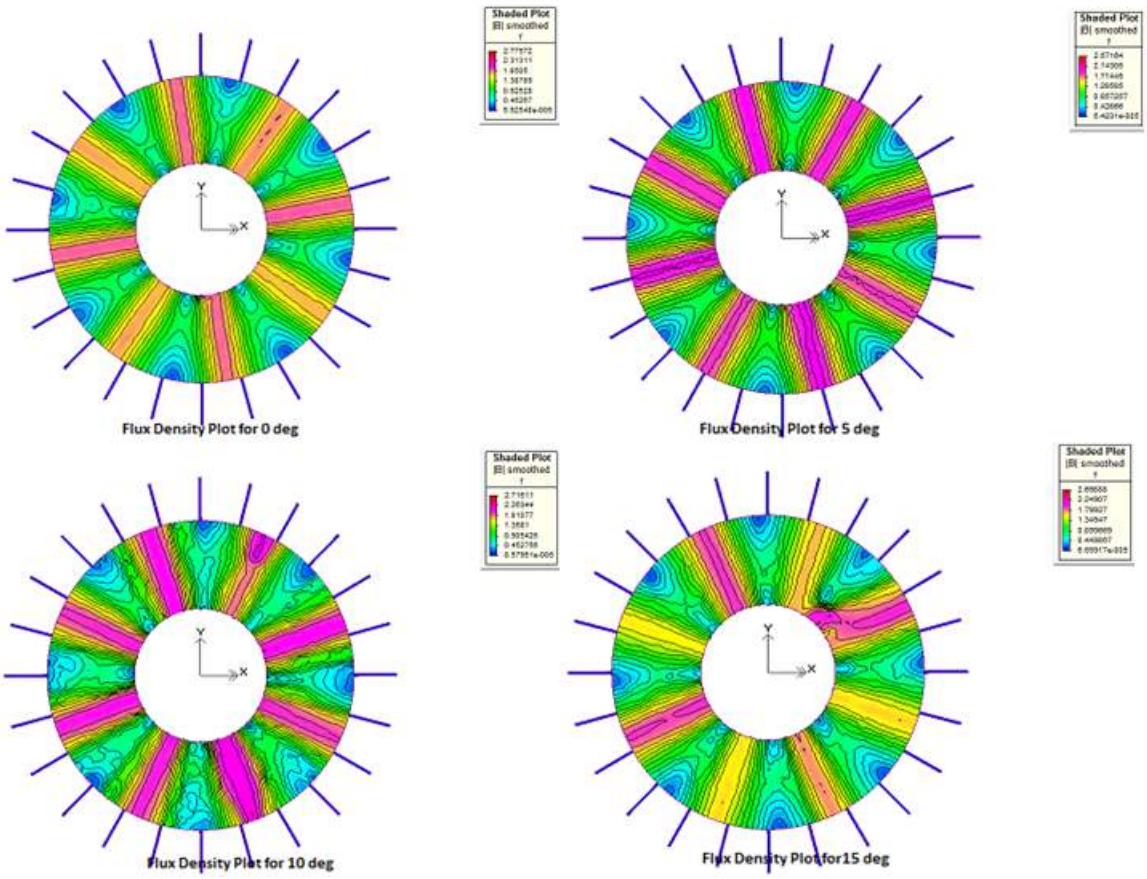

Figure 4.13: Flux density plot(B smoothed)

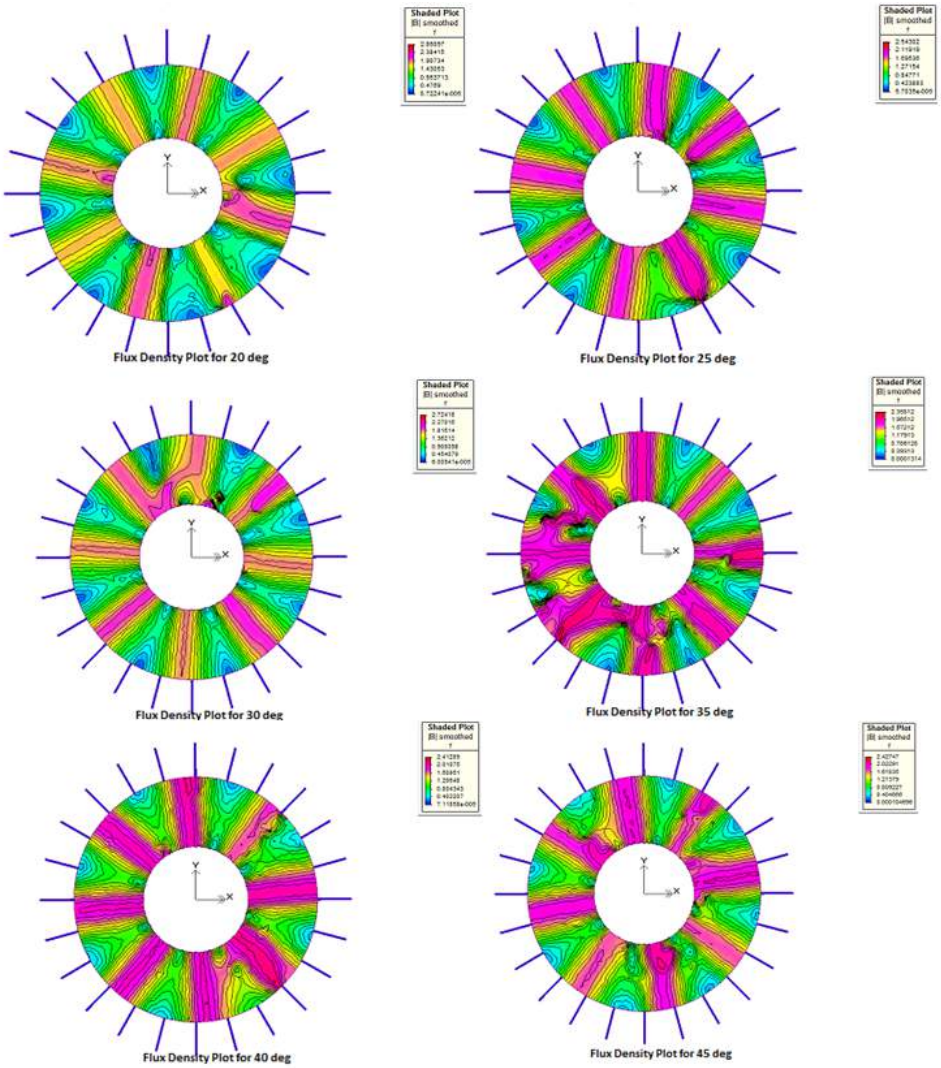

Figure 4.14: Flux density plot(B smoothed)

The plot for the B smoothed shaded and arrow plot can be seen in the following figure

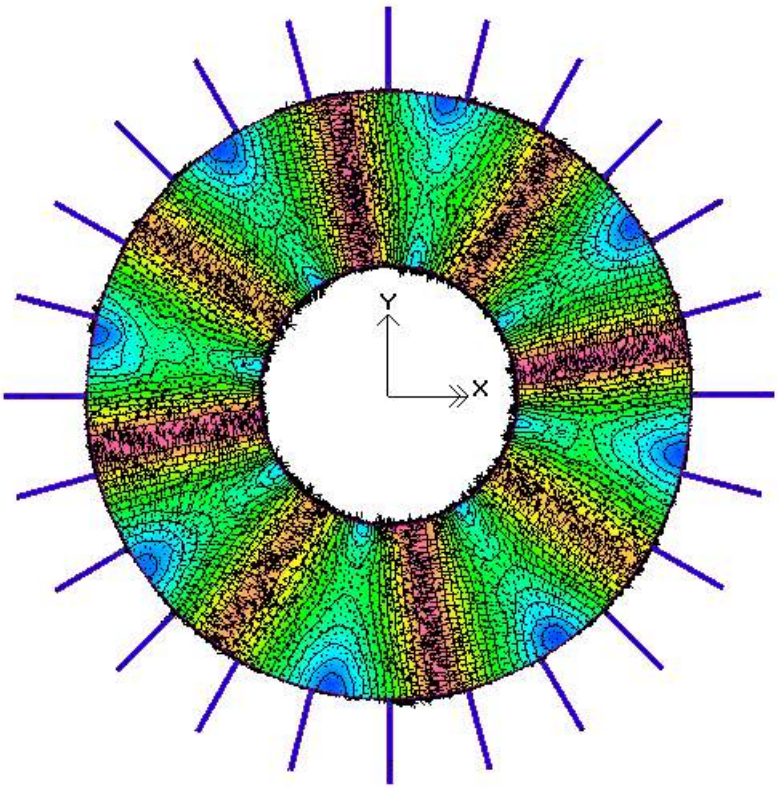

Figure 4.15: B smoothed Shaded and Arrow plot

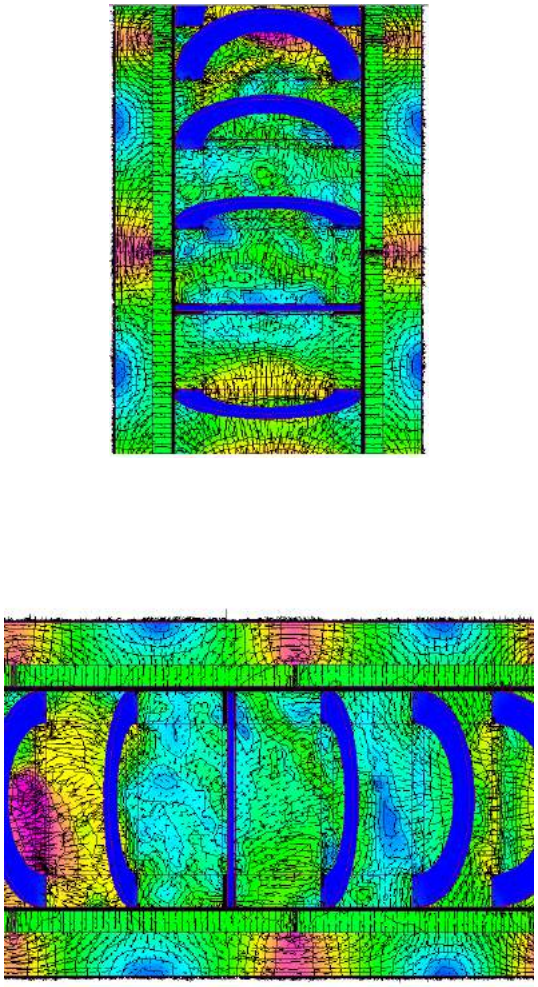

Figure 4.16: B smoothed Shaded and Arrow plot

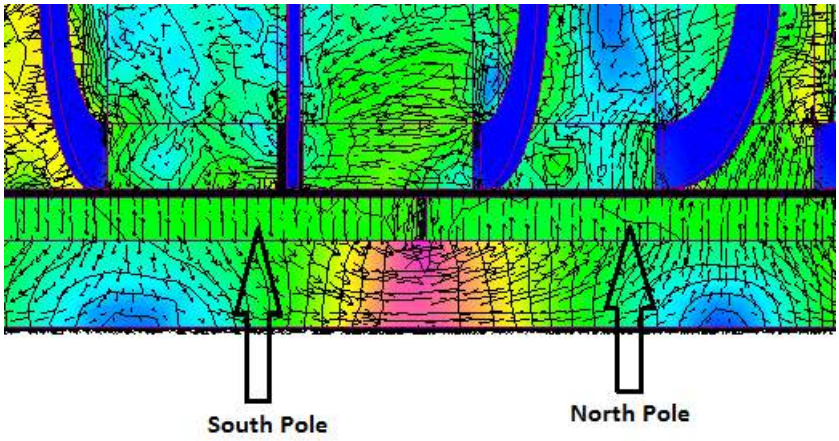

Figure 4.17: B smoothed Shaded and Arrow plot

It can be seen from the plot that the flux leave from the south pole and the enter the north pole

The following plot show the relative permability it can be seen that as the relative permeability of the permanent magnet is 1.

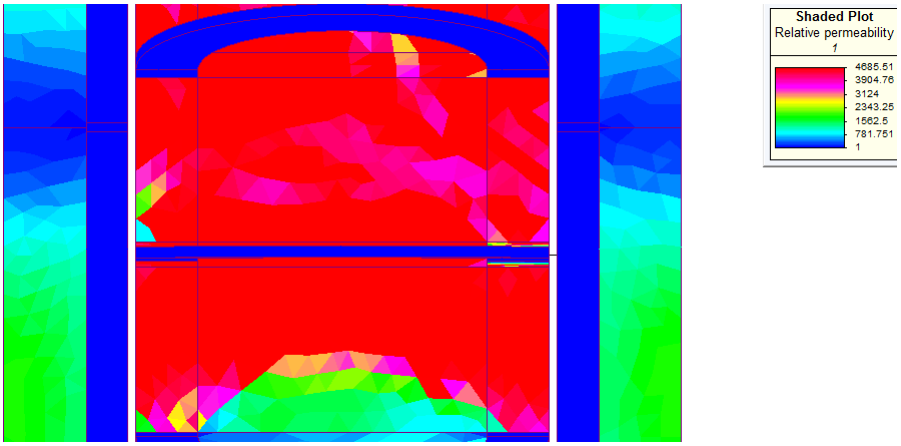

Figure 4.18: Plot for Relative Permeability

4.7 Comparison of CAD and FEA

Parameter	CAD	3D FEA
Average Flux Density(T)	0.75	0.83
Average Torque(Nm)	15.90	15.371
Torque Ripple		7.6%
Cogging Torque(Nm)		.99

4.8 2D Finite Element Analysis

An Axial field permanent magnet machine requires 3D Finite element analysis owing to its special construction, for accurately calculating its performance such as developed torque, etc. As axial flux machine can be analyzed in 2-D FE method by a novel integral force technique [11]. In this technique the 3 D model is cutting and stretching to a length equal to the circumference at the mean radius. Actually in axial flux motors, the flux density is not constant throughout the radial depth therefore; the force becomes a function of the radius as given in (4.1).

$$T = \int F dr \tag{4.1}$$

$$F = 2K_w N_m N_{spp} B_g n_s i r \tag{4.2}$$

The 2-D FE analysis can be carried out for motor in the radially cut and stretched formation. The current direction in each coil can be considered as radially inwards or outwards. In the radial cut for one pole pair, the direction of the current is considered as perpendicular to the X-Y plane. As the magnetic potential vector A is perpendicular to the sheet in the 2-D model the magnetic field will be lying within the X-Y plane. Hence, the 2-D analysis is valid for this case. For the technique considered the radial depth is divided in to 18 number of segments with equal radial

depth of 3mm for each segment. The radial segments are considered with some finite number and the force can be calculated on each segment. The integration of the force through the inner radius to the outer radius gives the total torque developed by the motor, as given in above equation. For different segments, the dimensions for the slot do not change along the radial depth. The width of the stator teeth is changing with the radius. The width of permanent magnet pole and the magnet spacer are changing with the radius. The 2-D FE model is prepared at the center of each segment. The accuracy of the analysis depends on number of segments. Then, 2-D FE analysis is carried out for each segment and the force is calculated for each segment. The force calculated by the FEA package is for the unit depth of the model. For each segment, the product is calculated using the force obtained from the 2-D FE analysis, depth of the segment, and the number of pole pairs.[8] For this technique equation(4.1) can be modified into

$$T = \sum_{i=1}^{n} dr \tag{4.3}$$

where n = number of segments

The inner and outer segment of the model is as shown in the figure 4.19 and 4.20

The torque obtained by this 2D finite element analysis method is 13.48056 Nm. Here time required for 2D analysis is less than the 3D finite element analysis but the accuracy is less. The accuracy increases with the increase in the number of segments.

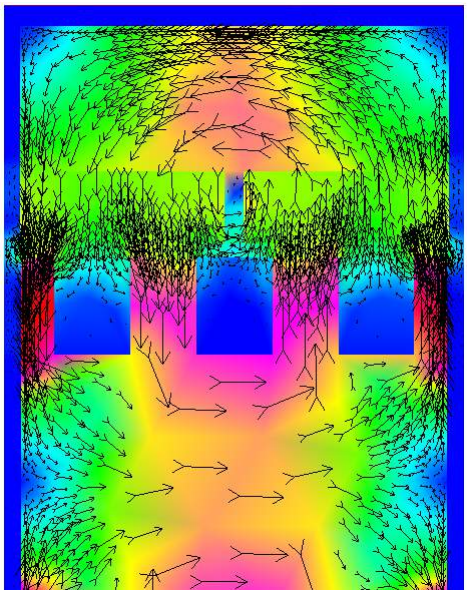

Figure 4.19: B smoothed Shaded and Arrow plot for inner radius

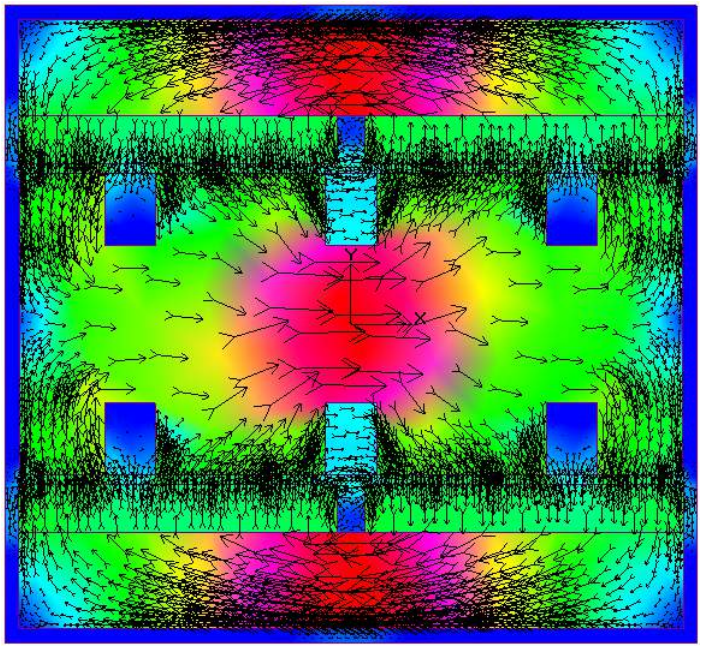

Figure 4.20: B smoothed Shaded and Arrow plot for outer radius

Chapter 5

Conclusion & Future Scope

5.1 Conclusion

Complete computer aided programming of the sandwiched stator dual air-gap axial flux PMBLDC motor of rating 250 Watt, 48 Volt and 150 RPM has been finalized. Based on this computer aided program output,model is prepared in Finite element software and analyzed. The computer aided program results are fairly matching with results obtained from Finite element analysis.

5.2 Future Scope

- Further refinement of the design can be done.
- Fabrication of hardware model of Axial flux permanent magnet brushless DC motor.
- Different test on motor for High and low load, pulsating load , variable load condition should be carry out.

References

[1] M. Aydin, S. Huang and T.A. Lipo ***"Axial Flux Permanent Magnet Disc Machines: A Review"*** In Conf. Record of SPEEDAM, Capri Italy, May 2004, pp. 61-71.

[2] P. R. Upadhyay, K. R. Rajagopal, and B. P. Singh ***"Computer aided design of an axial-field PM brushless DC motor for an electric vehicle"*** IEEE Transactons on magnetics, Vol. 42, No. 10, October 2006.

[3] T.J.E. Miller ***"Brushless Permanent Magnet and Reluctance Motor Drives, "*** Oxford University Press ,1989.

[4] A. Cavagnino, M. Lazzari, F. Profumo and A. Tenconi ***"A comparison between the axial flux and the radial flux structures for PM synchronous motors"*** IEEE Transactions on Industry Applications, Vol.38, No.6, Nov/Dec 2002., pp.1611-1618.

[5] D. C. Hanselman ***"Brushless Permanent Magnet-Motor Design."*** New York: McGraw-Hill, 1994 McGraw-Hill.

[6] Yon-Do Chun, Dae-Hyun Koo, Yun-Hyun Cho and Won-Young Cho ***"Cogging Torque Reduction in a Novel Axial Flux PM Motor"*** International Symposium on Power Electronics,SPEEDAM 2006.

[7] Jacek F. Gieras, Rong-Jie Wang and Maarten J. Kamper ***"Axial Flux Permanent Magnet Brushless Machines "*** 2005 Springer Science

[8] P. R. Upadhyay and K. R. Rajagopal ***"A Novel Integral-Force Technique for the Analysis of an Axial-Field Permanent-Magnet Brushless DC Motor Using FE Method"*** IEEE Trans. on Magnetics, vol. 41, 2005, pp. 3958-3961.

[9] Electric Motor ***"http://en.wikipedia.org."***